Theoretical Study of the Thermolysis of β-Hydroxyl Aldehydes

Norberto Castillo and Russell J. Boyd*

Department of Chemistry, Dalhousie University, Halifax, Nova Scotia, Canada B3H 4J3

Received: January 27, 2006; In Final Form: April 18, 2006

A mechanism involving a six-membered cyclic transition state where the hydrogen of the hydroxyl group interacts with the oxygen of the carbonyl group has been proposed previously to describe the thermolysis of many β-hydroxyl compounds. In this paper, the proposed mechanism is studied for a series of β-hydroxyl aldehydes. Rate constants and activation energies are reported as well as a study of the influence of tunneling on the reaction rates. The electron density at the ring critical points, population analyses by the theory of atoms in molecules (AIM) and the natural bond orbital (NBO) method, as well as atomic energy analyses are used to gain insight into this interesting mechanism and into the effects of substituents.

Introduction

The kinetics of the thermal decomposition of β-hydroxyl compounds have been characterized in many β-hydroxyl compounds. The first experimental studies were carried out by Smith and Yates[1] in 1965 and by Yates and Quijano[2] in 1969. The latter studied the thermal decomposition of β-hydroxy ketones and concluded that it is a first-order intramolecular reaction in which the hydrogen of the hydroxyl group interacts with the oxygen of the carbonyl group forming a six-membered cyclic transition state. Also, they analyzed the effect of replacing the hydrogens on the carbon adjacent to the hydroxyl group by methyl groups. The activation energies of alkyl β-hydroxy ketones were found to be about 30 kcal/mol, and the substitution of hydrogens by methyl groups was shown to accelerate the rate of the thermolysis.

Subsequent experimental and theoretical studies in the gas and solution phases have been reported for many β-hydroxy compounds such as β-hydroxyl ketones,[3] β-hydroxyl esters,[4−8] β-hydroxyl olefins,[9] and β-hydroxynitriles.[10−12] All studies also included alkyl β-hydroxyl compounds and arrived at the same conclusions as that of the primary ketone cases.

In this paper, we report a theoretical study on the thermolysis of a group of β-hydroxyl aldehydes at the MP2(FC)/6-31G(d) and B3LYP/6-31G(d) levels with the emphasis on the activation energies and rate constants obtained by using conventional transition state theory (TST).[13] Also, single-point calculations by both methods using the 6-311++G(d,p) basis set were performed for the reactants and transition states. We include alkyl β-hydroxyl aldehydes and chloro β-hydroxyl aldehydes in order to analyze substituent and electronic effects. Furthermore, the theory of atoms in molecules (AIM) is used to study the topology of the electronic structure along the reaction path and to gain insight into this interesting mechanism. The thermolysis for β-hydroxyl aldehydes has not been studied previously.

Theoretical Background

Transition State Theory. The TST formula to calculate the rate constant is

$$k = \kappa \frac{k_B T}{h} \frac{Q^{TS}}{Q^{React}} \exp\left(-\frac{E_a}{RT}\right) \quad (1)$$

where E_a is the activation energy; κ is the tunneling factor; k_B, h, and R are the Boltzmann, Planck, and universal gas constants, respectively. Q is the partition function, and T is the temperature.

The proposed mechanism for the thermolysis of β-hydroxyl aldehydes is unimolecular and does not involve radical species. Therefore, to calculate the partition function term it is only necessary to compute the rotational and vibrational partition functions because the electronic and translational partition functions[14] are the same for the reactant and transition state and therefore cancel. The equations to calculate the rotational and vibrational partition functions are as follow:

$$Q_R = \frac{1}{\sigma}\left(\frac{k_B T}{h}\right)^{3/2}\left(\frac{\pi}{ABC}\right)^{1/2} \quad (2)$$

$$Q_v = \prod_i \frac{1}{1 - \exp\left(-\frac{h\nu_i}{k_B T}\right)} \quad (3)$$

where σ is the symmetry number (which is equal to unity in our systems[13]); A, B, and C are the rotational constants; and υ is the vibrational frequency.

The tunneling factor calculations were carried out by assuming unsymmetrical Eckart barriers.[15,16] In essence, the calculation of the tunneling factor in terms of Eckart barriers (which mainly depend on the imaginary frequency of the transition state among other parameters such as the reaction temperature, activation energy, and enthalpy of reaction) is an improved version of the simplest methods of Wigner[17] and the parabolic-type barrier tunneling corrections.[18] The Eckart barrier tunneling calculation is still widely used even though more sophisticated tunneling methods such as the multidimensional semiclassical zero and small-curvature methods[19] have been proposed. In 1997 Truong demonstrated the fairly good accuracy of the Eckart barrier tunneling calculation in his study of the hydrogen exchange reaction of methane in a zeolite.[20,21]

AIM Theory. According to the theory of atoms in molecules,[22−25] a molecule can be partitioned into atomic regions (basins) by zero-flux surfaces that satisfy the quantum condition:

$$\nabla\rho(\mathbf{r})\cdot\mathbf{n}(\mathbf{r}) = 0 \quad \text{for all } \mathbf{r} \text{ on the surface} \quad (4)$$

where $\nabla\rho(\mathbf{r})$ is the gradient of the electron density and $\mathbf{n}(\mathbf{r})$ is a unit vector normal to the surface. The many atomic properties

* Corresponding author. Tel.: (902)494-3305. Fax: (902)494-1310. E-mail: russell.boyd@dal.ca.

10.1021/jp060599a CCC: $33.50
Published on Web 06/20/2006

that are well-defined and can be computed for each basin provide important insight into the electronic structure of molecules. For example, the atomic population ($N(\Omega)$), which is determined by the integration of ρ over the basin of the atom of interest, is given by

$$N(\Omega) = \int_{\Omega} \rho(\mathbf{r})\, d\mathbf{r} \tag{5}$$

Several other properties such as atomic kinetic energies and the atomic dipolar polarization are calculated in a similar way. For example, the atomic dipolar polarization (or first atomic electrostatic moment) is given by

$$\mathbf{M}_1(\Omega) = -e\int_{\Omega} \mathbf{r}_{\Omega}\rho(\mathbf{r})\, d\mathbf{r} \tag{6}$$

where e is the elementary charge.

Furthermore, the determination of the critical points and their properties in the topology of ρ can provide much information about molecular systems. Each critical point is characterized by its rank and signature.[23,24] The rank is determined by the number of nonzero eigenvalues (or curvatures) of the associated Hessian matrix. The signature is the algebraic sum of the signs of the eigenvalues; a positive eigenvalue indicates that the function is a minimum in the direction defined by the eigenvector, and a negative sign indicates the opposite. There are four types of critical points in the electron density of molecular systems: nuclear $(3, -3)$, bond $(3, -1)$, ring $(3, +1)$, and cage $(3, +3)$. Bond critical points appear between two bonded atoms and are indicative of the existence of a chemical bond. Ring critical points appear in the center of cyclic structures, and cage critical points appear inside all chemical structures that engulf a volume in space.

NBO Analysis. Natural bond orbital (NBO) analysis is a powerful tool to characterize bonds, hyperconjugation effects, bond polarization, hybridization, and atomic populations in molecules.[8,26−28] The NBO population analysis is carried out in terms of natural atomic orbitals (NAOs), which are the eigenvectors $\{\varphi_i\}$ obtained by the diagonalization of the atomic one-center blocks of the one-particle density operator expressed in an AO basis $\{\phi_i\}$. Therefore, the matrix representation of the one-particle density operator expressed in the basis of NAOs is a diagonal matrix whose diagonal elements are the orbital populations:

$$p_i^{(A)} = \int \varphi_i^{(A)*}(1)\hat{\gamma}(1|1')\varphi_i^{(A)}(1')\, d\tau_1\, d\tau_{1'} \tag{7}$$

The NBO atomic populations are given by

$$p^{(A)} = \sum_i p_i^{(A)} \tag{8}$$

where the summation extends over all NAOs on center A.

Computational Details

The optimization of the geometries of the reactants and products and the exploration of the potential energy hypersurface to determine the transition states and the reaction paths were carried out at MP2(FC) and B3LYP/6-31G(d) levels of theory. Single-point calculations at MP2(FC) and B3LYP/6-311++G(d,p) were also carried out. The ab initio calculations were performed by using the GAUSSIAN 03 computational package.[29] Intrinsic reaction coordinate (IRC) calculations were carried out to ensure the validity of the stationary points found (reactants, transition states, and products). The energy barriers are corrected for the zero-point vibrational energy (ZPVE). A modified version of the numerical integration program of Brown[30] was used for the calculation of the tunneling factors.

The characterization of critical points was performed using the EXTREME program. The PROAIM program was used to compute the atomic populations, atomic dipole moments and atomic energies. Both programs belong to the AIMPAC package.[31]

Results and Discussion

Transition State Characterizations and Determination of Kinetic Parameters. The mechanism suggested for the thermolysis of the β-hydroxyl aldehydes is shown in Figure 1. It is very similar to those proposed for other β-hydroxyl compounds. Table 1 lists the bond distances in the reactants and the transition states at the MP2(FC)/6-31G(d) level for several β-hydroxyl aldehydes.

The O_1-C_2 distance and the C_4-O_5 distance increase and decrease, respectively, from the reactants to the transition states in all systems, representing the transition from a CO double bond to a CO single bond and from a CO single bond to a CO double bond, respectively. In all transition states, H_6 is closer to O_1 than to O_6; therefore, they can be classified as late transition states. Furthermore, Table 1 shows that the C_3-C_4 distance increases from the reactants to the transition states for all systems, indicating the breaking of this bond.

Quijano et al.[9] observed nearly planar transition states in their study of β-hydroxyl olefins, whereas the six-membered cyclic transition states in our systems are far from planarity. The dihedral angles of the transition states are shown in Table 2. The $C_2-C_3-C_4-O_5$, $C_4-O_5-H_6-O_1$, and $O_1-C_2-C_4-O_5$ dihedral angles for system 7 are very different from the average values for the other of β-hydroxyl aldehydes. This fact will be discussed below.

In general, the kinetics parameters of the ketones and aldehydes are very similar, which is not surprising because they are both classified as being carbonyl compounds. Experimental data for the thermolysis of β-hydroxyl aldehydes is unavailable. Therefore, we use the experimental activation energies and rate constants for β-hydroxyl ketones to compare with those of the β-hydroxyl aldehydes. In our work the activation energies and rate constants for some alkyl β-hydroxyl ketones[2] at 206.5 °C were used for the comparison; thus, the rate constants for the β-hydroxyl aldehydes were calculated at this temperature.

The activation energies and the rate constants for the alkyl-substituted β-hydroxyl ketones are about 31 kcal/mol and 10^{-4} s^{-1}, respectively. The proposed mechanism (Figure 1) involves the interaction between the hydrogen of the hydroxyl group and an electron pair of the carbonyl oxygen to form a six-membered cycle. The β-hydroxyl ketones should have lower activation energies and greater rate constants than the β-hydroxyl aldehydes because the electron pair on the carbonyl oxygen is more available in the ketone case due to the positive inductive effect of the methyl group. The chlorine-substituted β-hydroxyl aldehydes were included to analyze the influence of the negative inductive effect in this mechanism. Furthermore, we analyzed β-hydroxy aldehydes substituted at C_3 and C_4 to determine which position produces a larger contribution.

Table 3 summarizes the activation energies and the rate constants (not corrected by the tunneling factor) for the thermolysis of β-hydroxy aldehydes at 206.5 °C obtained with MP2(FC)/6-311++G(d,p)//MP2(FC)/6-31G(d) and B3LYP/6-311++G(d,p)//B3LYP/6-31G(d).

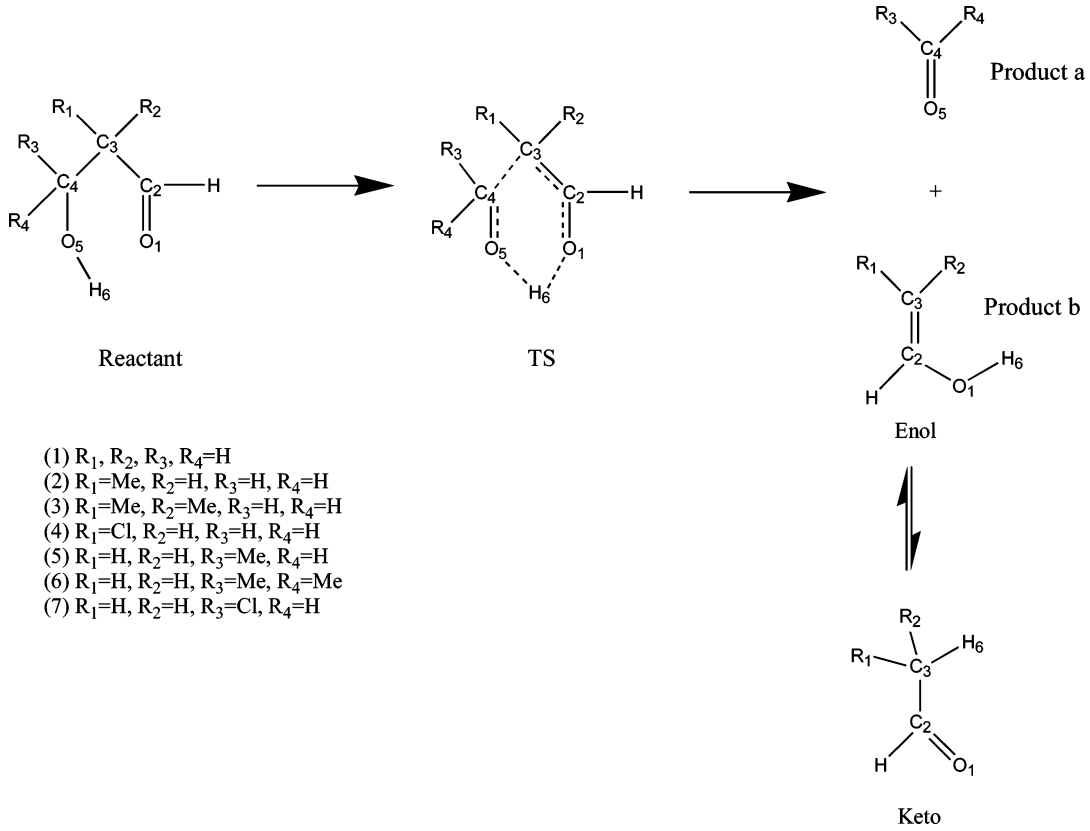

Figure 1. Mechanism for the thermolysis of β-hydroxyl aldehydes: (1) β-hydroxyl aldehyde, (2) 3-methyl β-hydroxyl aldehyde, (3) 3,3-dimethyl β-hydroxyl aldehyde, (4) 3-chloro β-hydroxyl aldehyde, (5) 4-methyl β-hydroxyl aldehyde; (6) 4,4-dimethyl β-hydroxyl aldehyde, (7) 4-chloro β-hydroxyl aldehyde.

TABLE 1: MP2(FC)/6-31G(d) Bond Distances (Å) of the Optimized Structures of Reactants and Transition States of β-Hydroxyl Aldehydes

structure	O_1-C_2	C_2-C_3	C_3-C_4	C_4-O_5	O_5-H_6	H_6-O_1
reactant-1	1.223	1.508	1.525	1.428	0.973	3.535
TS-1	1.303	1.386	2.012	1.282	1.386	1.105
reactant-2	1.223	1.510	1.526	1.426	0.973	3.485
TS-2	1.304	1.388	2.017	1.283	1.358	1.108
reactant-3	1.223	1.515	1.532	1.425	0.972	3.718
TS-3	1.306	1.392	2.045	1.285	1.347	1.120
reactant-4	1.220	1.515	1.526	1.420	0.973	3.464
TS-4	1.299	1.388	2.033	1.279	1.343	1.117
reactant-5	1.223	1.508	1.529	1.432	0.974	3.440
TS-5	1.301	1.386	2.038	1.287	1.339	1.123
reactant-6	1.225	1.507	1.542	1.437	0.975	3.039
TS-6	1.300	1.386	2.065	1.293	1.306	1.142
reactant-7	1.222	1.512	1.521	1.392	0.976	3.369
TS-7	1.299	1.394	1.910	1.260	1.453	1.072

The MP2 activation energies and rate constants are about 5 kcal/mol greater and 1 order of magnitude less, respectively, than the experimental results of similar β-hydroxyl ketones. Table 3 also illustrates the same trends for the substitution in every position except the case of chlorine at C_4 (system 7). The β-hydroxyl aldehyde with chlorine substituted at C_4 has a lower activation energy and greater rate constant, respectively, than the unsubstituted β-hydroxyl aldehyde (this fact will be analyzed in detail below by use of AIM theory). These results suggest that a positive inductive effect accelerates the reaction.

The MP2 results in Table 3 show that the thermolysis of a β-hydroxyl aldehyde substituted at C_4 exhibits a lower activation energy than with the same substituent substituted at C_3. This result is expected because C_4 is bonded directly to the oxygen of the hydroxyl group, which donates the hydrogen atom. When the oxygen atom begins to donate the hydrogen atom, the s character of the oxygen valence shell increases, and the oxygen atom becomes even more electronegative,[32−36] withdrawing electron density from the carbon. Therefore, a positive inductive effect at C_4 plays a larger role in the thermolysis than at C_3 because the positive character at C_4 is greater than at C_3. This point is supported by the population analysis presented in the following section.

The B3LYP barriers are much lower (by as much as 6 kcal mol^{-1}); therefore, the B3LYP rate constants are much higher. This is similar to the results for β-hydroxyl olefins, for which Quijano et al.[9] concluded that B3LYP overestimates the rate constants.

Even though it is well-known that the tunneling factor decreases as the temperature increases,[18] the analysis of tunneling gives information about the barrier shape and also contributes to the analysis of substituents effects.[37] Table 4 reports the tunneling factors as well as the corrected rate constants for the thermolysis of the seven systems at 206.5 °C at the MP2(FC)/6-311++G(d,p)//MP2(FC)/6-31G(d) level.

According to the tunneling criteria given by Bell [$1 < \kappa < 1.1$, negligible tunneling; $1.1 < \kappa < 4$, small to moderate tunneling; and $4 < \kappa$, large tunneling[18]], the thermolysis of β-hydroxyl aldehydes exhibits small tunneling factors and does not produce changes in the order obtained from the uncorrected rate constants. Moreover, the tunneling factors show clearly the positional dependence of substituent effects. For instance, methyl at C_3 (systems 2 and 3) leads to tunneling factors smaller than the unsubstituted β-hydroxyl aldehyde, whereas at C_4 (systems 5 and 6) the tunneling factors are greater than in the unsubstituted aldehyde. However, when the substituent is chlorine the opposite effect is observed: systems 4 and 7 exhibit smaller and larger tunneling factors than the unsubstituted aldehyde, respectively.

TABLE 2: MP2(FC)/6-31G(d) Dihedral Angles (in deg) of Transition States of β-Hydroxyl Aldehydes

	dihedral angles (°)					
TS	$O_1-C_2-C_3-C_4$	$C_2-C_3-C_4-O_5$	$C_3-C_4-O_5-H_6$	$C_4-O_5-H_6-O_1$	$O_1-C_2-C_4-O_5$	$C_2-C_4-O_5-H_6$
TS-1	−61.0	58.8	−30.5	−9.2	7.4	−2.2
TS-2	−62.2	56.5	−27.9	−10.9	4.2	−0.1
TS-3	−67.9	60.6	−32.7	0.2	4.4	−2.5
TS-4	−60.5	58.6	−31.3	−2.7	6.9	−3.2
TS-5	−59.5	59.0	−32.2	−5.5	9.7	−4.2
TS-6	−58.8	58.8	−33.0	−2.3	10.7	−5.4
TS-7	−57.0	46.5	−12.9	−39.9	−2.5	10.2

TABLE 3: MP2(FC)/6-311++G(d,p)//MP2(FC)/6-31G(d) and B3LYP/6-311++G(d,p)//B3LYP/6-31G(d), Activation Energies and Rate Constants of β-Hydroxyl Aldehydes

activation energy (kcal mol^{-1})			rate constant (s^{-1})	
system	MP2	B3LYP	MP2 × 10^5	B3LYP × 10^3
1	36.3	31.1	3.566	8.373
2	35.1	29.3	19.001	83.311
3	34.8	29.3	36.109	100.895
4	37.8	31.3	0.861	8.112
5	35.0	29.0	17.872	99.801
6	33.0	26.3	99.974	1641.995
7	36.0	30.0	5.476	31.859

TABLE 4: MP2(FC)/6-311++G(d,p)//MP2(FC)/6-31G(d) Tunneling Factors and Corrected Rate Constants of β-Hydroxyl Aldehydes

system	tunneling factor (κ)	rate constant (s^{-1}) × 10^5
1	1.435	5.117
2	1.406	26.715
3	1.373	49.578
4	1.513	1.303
5	1.604	28.667
6	1.780	177.954
7	1.277	6.993

TABLE 5: MP2(FC)/6-311++G(d,p) Electron Densities and Eigenvalues at the Ring Critical Points of β-Hydroxyl Aldehydes

		Eigenvalue × 10^2		
system	$\rho \times 10^2$	1	2	3
1	2.28	−1.91	6.63	8.94
2	2.32	−2.00	6.56	9.21
3	2.50	−2.26	6.59	10.00
4	2.27	−1.92	6.48	8.91
5	2.26	−1.84	6.53	8.67
6	2.28	−1.82	6.39	8.56
7	2.21	−1.72	6.88	8.53

AIM Analysis. To determine if the reactions occur through a six-membered cyclic transition state, a topological study in terms of ring critical points was performed. Table 5 characterizes the ring critical points found for all the transition states. Figure 2 shows the molecular graphs and the location of the RCPs and their three respective eigenvectors for the seven systems. In all cases eigenvector 1 is nearly perpendicular to the six-membered ring. This shows that ρ is decreasing from the center of the ring in the perpendicular direction. Moreover, substitution at C_4 decreases the curvature of ρ in the direction perpendicular to the ring (eigenvalue 1), indicating a greater accumulation of ρ in the perpendicular direction for systems 5−7 than for the rest of the systems.

The electron density at the ring critical point (ρ_{RCP}) can be considered to be a criterion to measure how much a substituent stabilizes or destabilizes the transition state. For example, higher density at the RCP means stronger attractive interactions between the nuclei and the electron density, which in effect reduces the repulsion between nuclei and helps to stabilize the transition state. The ρ_{RCP} data yield the same trends as kinetics parameters for substituents at C_3. For example, system 3 exhibits the largest value of ρ at the ring critical point and the lowest activation energy while the opposite occurs with system 4. However, the same trend is not observed with substituents at C_4. Systems 5 and 6 exhibit very similar ρ_{RCP} to that of system 1 even though their activation energies are considerably lower. Also, system 7 exhibits lower ρ_{RCP} than system 1 even though its activation energy is lower. Moreover, this criterion does not reproduce the trends when the same substituent is at a different position (C_3 and C_4). For example, systems 2 and 3 exhibit larger ρ_{RCP} than systems 5 and 6, respectively, even though their activation energies are higher. These results also indicate that substituents at positions C_3 and C_4 play different roles in the thermolysis of β-hydroxyl aldehydes.

The electrostatic interaction between O_1 and H_6 in the reactants should contribute to the formation of the cyclic transition state. Therefore, it is reasonable to expect a greater electrostatic attraction between these two atoms would accelerate the reaction. For this reason, we calculated, as a first approximation, a point-charge interaction energy, $U_{PC} = q_{O_1}q_{H_6}/(d_{O_1-H_6})$, from the NBO and AIM charges and the internuclear distance (Figure 3). Table 6 lists the computed U_{PC} values.

The NBO charges differ considerably from those calculated by AIM. For example, the NBO charges of O_1 are roughly half of the AIM values. However, both methods yield similar trends. The NBO U_{PC} values for β-hydroxyl aldehydes substituted at C_3 and C_4 follow the trends 2 > 1 > 4 > 3 and 6 > 7 > 5 > 1, respectively, whereas the AIM values yield 2 > 4 > 1 > 3 and 6 > 7 > 5 > 1, respectively. As suggested above, a larger negative value of U_{PC} indicates a greater attractive interaction; therefore, it should correlate with faster thermolysis. The results shown in Table 6 reproduce the trend obtained by analyzing the kinetics parameters for β-hydroxyl aldehydes substituted at C_4 except that the thermolysis of system 5 (U_{PC}(NBO) = −20.8 kcal/mol, U_{PC}(AIM) = −56.1 kcal/mol) is faster than that of system 7 (U_{PC}(NBO) = −21.3 kcal/mol, U_{PC}(AIM) = −58.9 kcal/mol). Furthermore, the U_{PC} values for β-hydroxyl aldehydes substituted at C_4 are more negative than the respective ones substituted at C_3; therefore, their thermolysis reactions are faster, which is consistent with the kinetics parameters (Table 3). The U_{PC} values for β-hydroxyl aldehydes substituted at C_3 do not reproduce the trend obtained by analyzing the kinetics parameters (Table 3).

As a second approximation, we calculated the dipole−moment interaction energy (U_{DM}) between the two atomic dipole moments of O_1 and H_6. Figure 4 indicates the direction of the atomic dipole moments of O_1 and H_6 in system 1. Similar directions were found for the other systems. We used the standard equation which describes the interaction energy between two dipole moments:[38]

$$U_{DM} = \frac{[\mathbf{M}_1(O_1)\cdot\mathbf{M}_1(H_6) - 3(\mathbf{M}_1(O_1)\cdot\hat{\mathbf{d}}_{O_1-H_6})(\mathbf{M}_1(H_6)\cdot\hat{\mathbf{d}}_{O_1-H_6})]}{d^3_{O_1-H_6}} \quad (9)$$

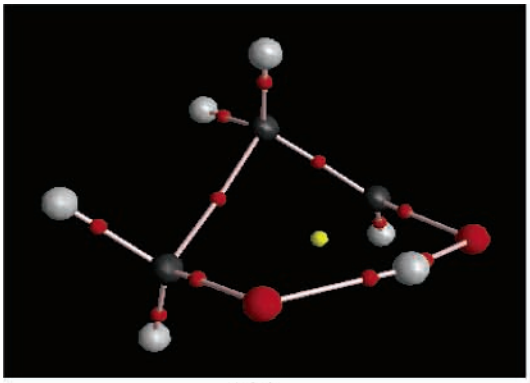

1(a)

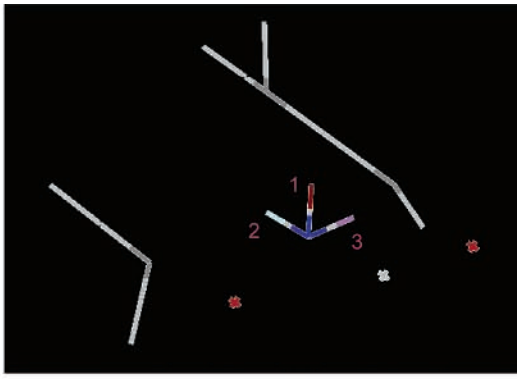

1(b)

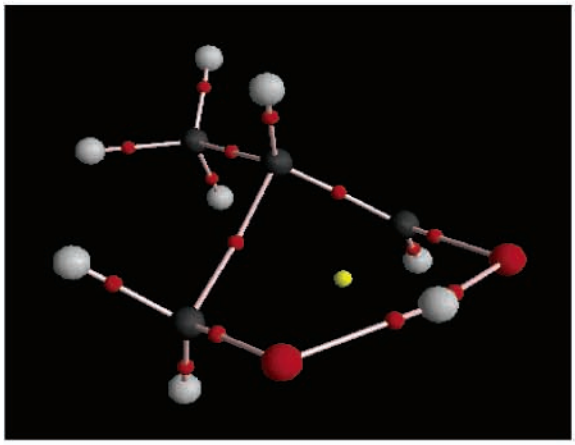

2(a)

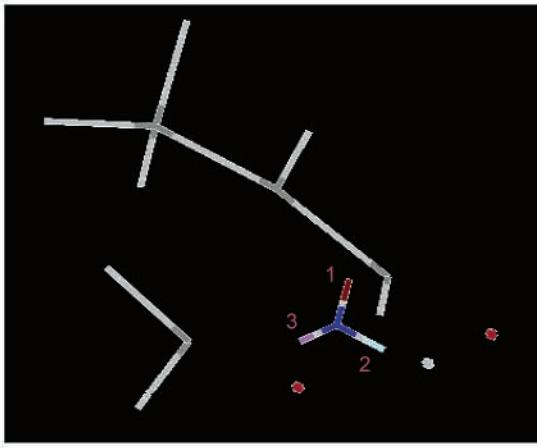

2(b)

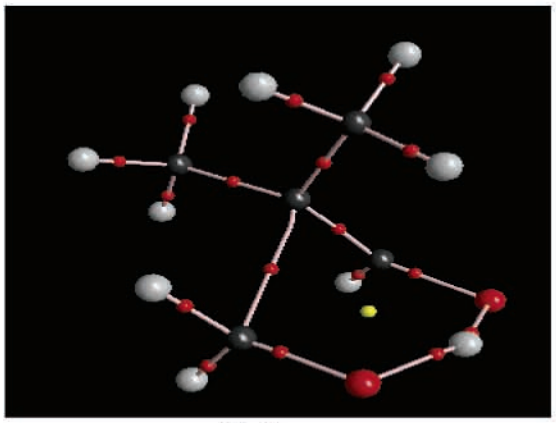

3(a)

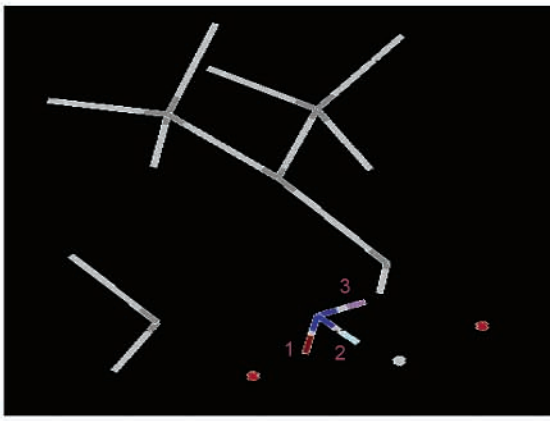

3(b)

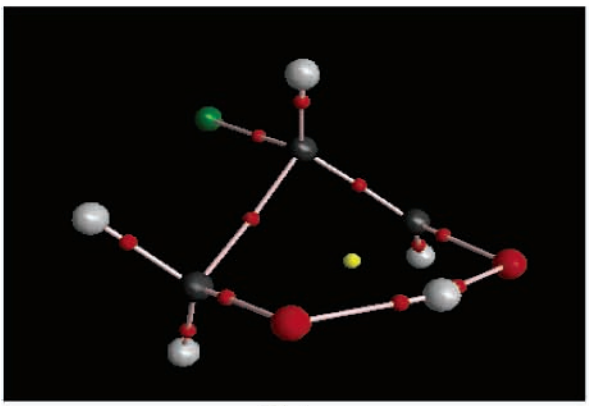

4(a)

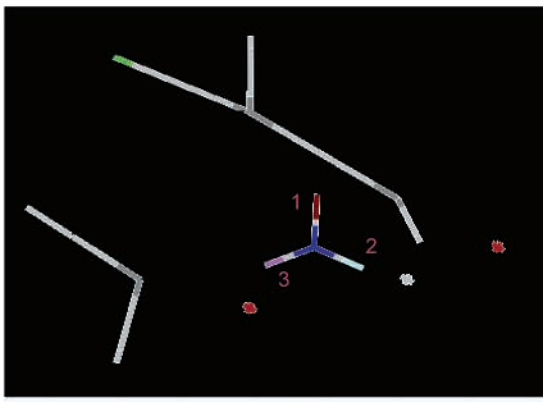

4(b)

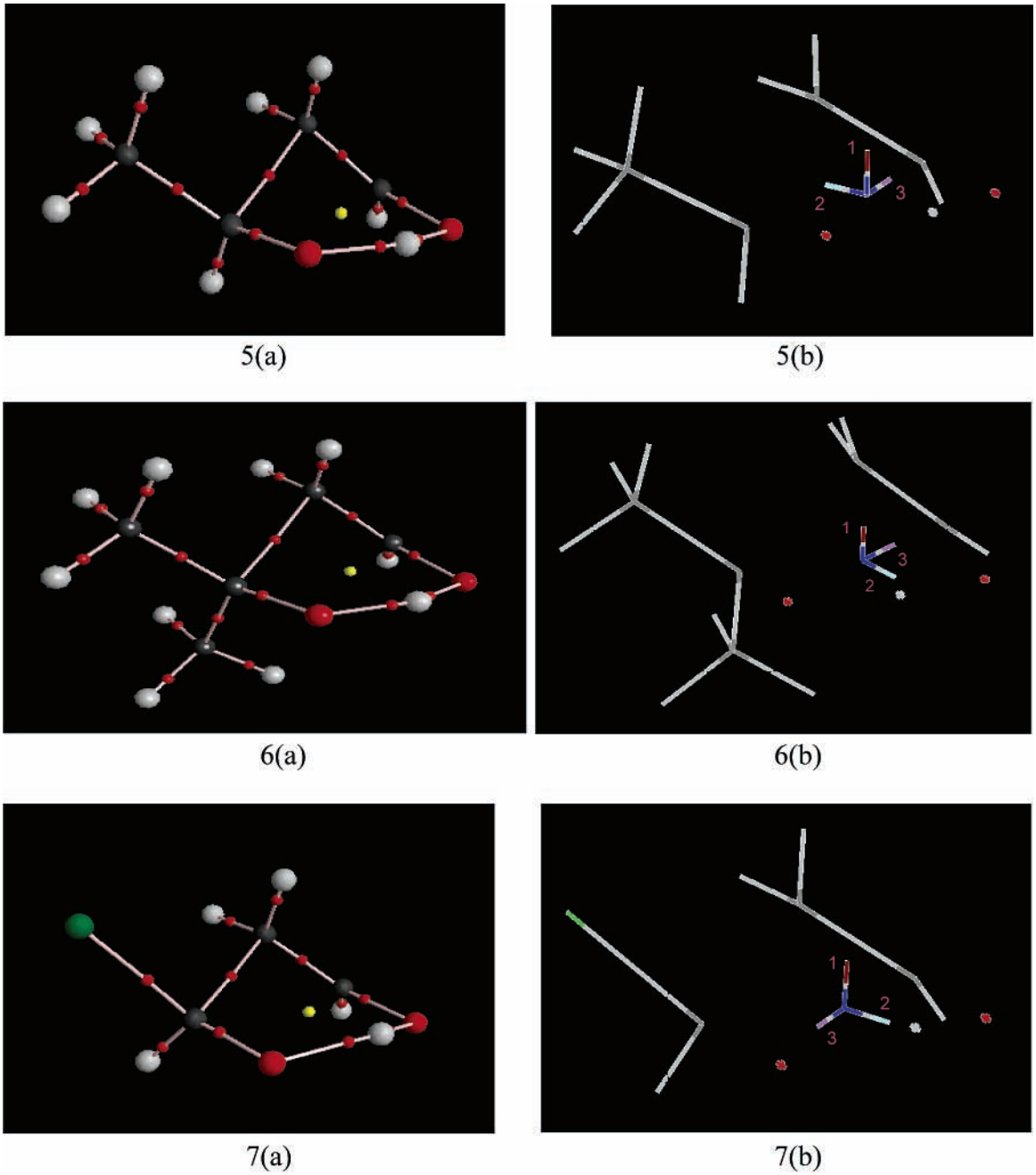

Figure 2. (a) Molecular graphs of the transition states of β-hydroxyl aldehydes. BCPs and RCPs are denoted by red and yellow dots, respectively. (b) Characterization of the ring critical points and the eigenvectors in the transition states of β-hydroxyl aldehydes. The seven systems are defined in Figure 1, and eigenvectors are indicated in order of increasing eigenvalues in accordance with Table 5.

where $\mathbf{M}_1(O_1)$ and $\mathbf{M}_1(H_6)$ are the atomic dipole moments of O_1 and H_6, respectively; $\hat{\mathbf{d}}_{O_1-H_6}$ is the unitary vector that defines the line connecting O_1 and H_6; and $d_{O_1-H_6}$ is the distance between O_1 and H_6. Table 7 lists U_{PC} and U_{DM} and the total interaction energies (U_{total}) for the seven systems.

The data in Table 7 shows that U_{total} and U_{PC} lead to the same trend and that the inclusion of U_{DM} has no effect on the trend. This suggests that the inclusion of higher electric moments would have a negligible effect.

The theory of atoms in molecules partitions a molecule into atomic fragments and yields an atomic energy associated with each atom. Changes in atomic energies can be used to determine the effect of substituents. Figure 5 illustrates the differences in atomic energies between transition states and reactants for all atoms that form the six-membered cyclic transition state. A negative value indicates a stabilization of the atom in the transition state with respect to the reactant, whereas a positive value indicates the opposite.

Comparison of systems 1−3 indicates that the atomic energy of C_3 is lowered substantially by successive methyl substituents at C_3. In the case of system 4, the atomic energy of C_3 (4.8 kcal/mol) is similar to that of system 1 (8.5 kcal/mol), but the stabilization of C_2 in system 1 (−115.9) is greater by almost 9 kcal/mol than in system 4 (−107.1 kcal/mol). Therefore, chlorine at C_3 stabilizes C_2 less with respect to the unsubstituted β-hydroxyl aldehyde, and it accounts primarily for the overall destabilization of the transition state relative to the reactant introduced by the negative inductive effect of chlorine. With respect to β-hydroxyl aldehydes substituted at C_4, the stabilization introduced by the positive inductive effect of the methyl group in system 5 relative to system 1 occurs mainly at O_5. Moreover, C_4 and O_5 are more stable in system 6 than in system

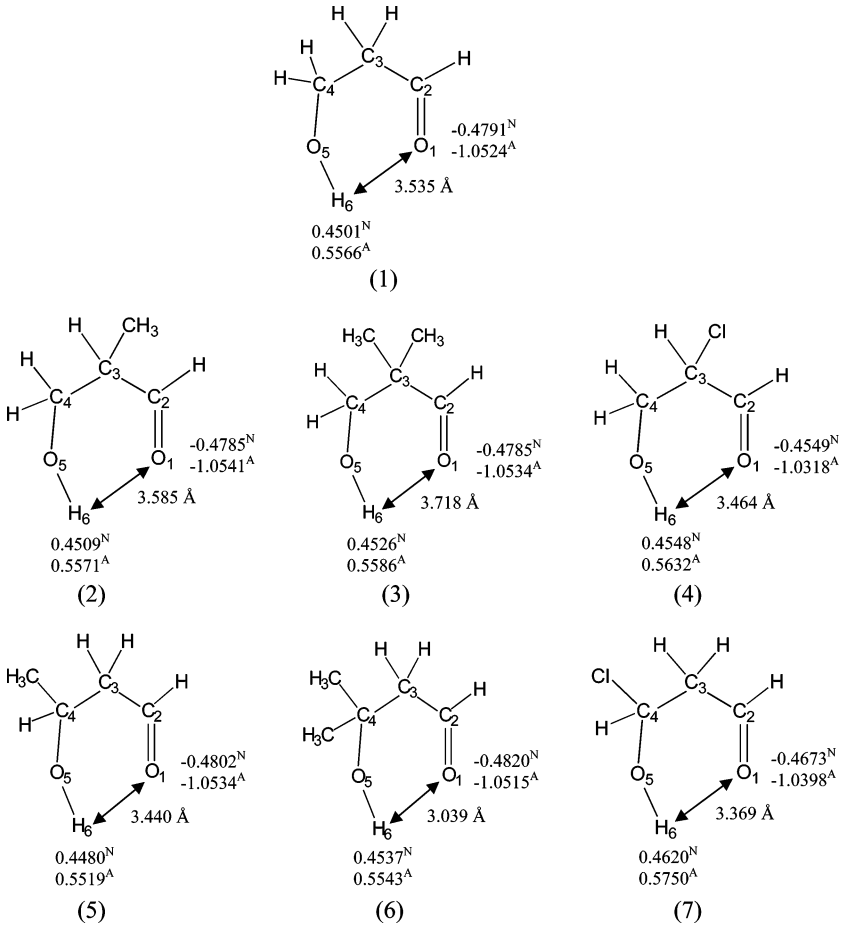

Figure 3. NBO (N) and AIM (A) atomic charges (au) as well as the interatomic distances (Å) between O_1 and H_6 for reactants of all the systems.

TABLE 6: Point Charge Contribution to the Interaction Energy (U_{PC}) (in kcal/mol) Obtained by NBO and AIM Analyses at the MP2(FC)/6-311++G(d,p) Level

system	NBO	AIM
1	−20.3	−55.0
2	−20.6	−56.0
3	−19.3	−52.6
4	−19.8	−55.7
5	−20.8	−56.1
6	−23.9	−63.7
7	−21.3	−58.9

TABLE 7: Point Charge Contribution (U_{PC}) and Dipole Moment Contribution (U_{DM}) to Total Interaction Energy (U_{total}) Obtained by AIM at the MP2(FC)/6-311++G(d,p) Level[a]

system	U_{PC}	U_{DM}	U_{total}
1	−55.0	0.3	−54.7
2	−56.0	0.3	−55.6
3	−52.6	−0.5	−53.0
4	−55.7	0.3	−55.4
5	−56.1	0.2	−56.0
6	−63.7	0.0	−63.6
7	−58.9	−0.3	−59.2

[a] The values are reported in kcal/mol.

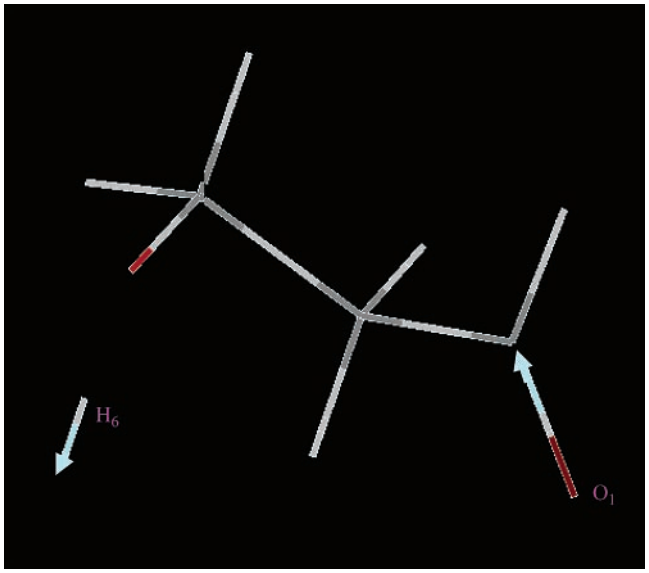

Figure 4. Directions of the atomic dipole moments of O_1 and H_6 in system 1.

1. On the other hand, system 7 exhibits a very unstable C_4 with respect to system 1; the negative inductive effect of chlorine produces a large destabilization of C_4. It is interesting to note that system 7 exhibits a much greater stabilization of O_1 at the transition state relative to the reactant than the rest of the systems.

Anomalous Behavior of 4-Chloro β-Hydroxyl Aldehyde. 4-Chloro β-hydroxyl aldehyde behaves differently from the other six systems. For example, the dihedral angles of the transition state of 4-chloro β-hydroxyl aldehyde are very different from the average of the other systems. Also, the tunneling factor is very different. Moreover, it has the lowest ρ_{RCP} at the transition state, and it has larger U_{PC} values (NBO and AIM) as well as U_{total} (AIM) than the other systems with the exception of 4,4-dimethyl β-hydroxyl aldehyde. Finally, 4-chloro β-hydroxyl aldehyde exhibits a much greater stabilization of O_1 in the transition state relative to the reactant than the rest of the

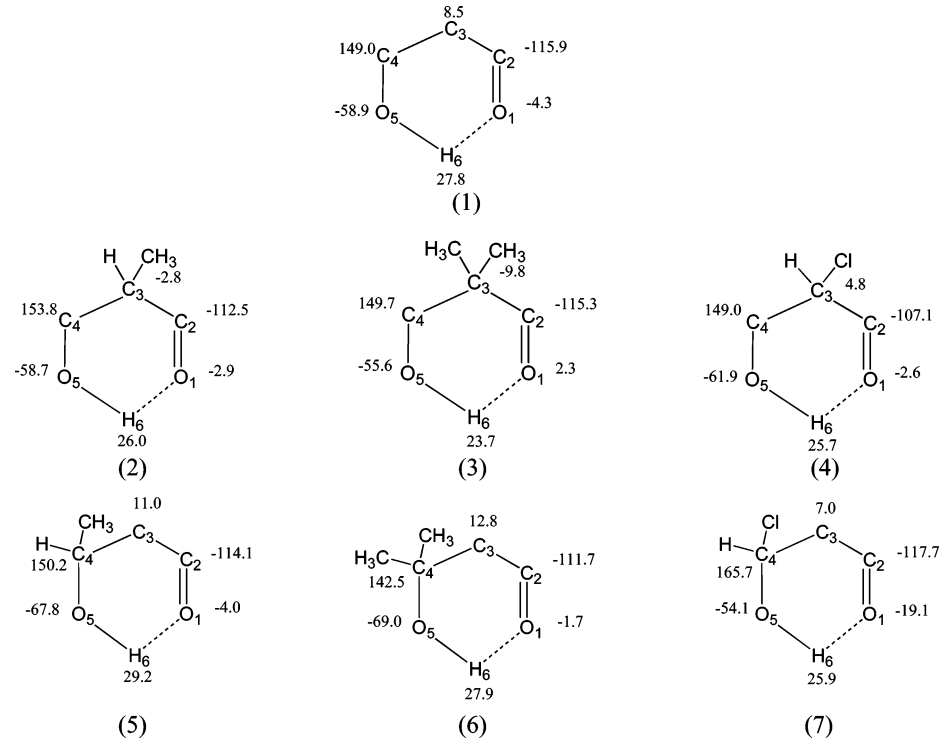

Figure 5. Differences in atomic energies (kcal/mol) between transition states and reactants for the atoms that form the six-membered cyclic transition state. For clarity, the substituents have been removed except at C_3 for systems 2, 3, and 4 and at C_4 for systems 5, 6, and 7.

systems. All these results indicate clearly that a chlorine at C_4 plays a totally different role than a chlorine at C_3 in the thermolysis of β-hydroxyl aldehydes. The effect of chlorine at C_3 is very different from that at C_4, which is bonded to an oxygen that is transformed from a single to a double bond during the reaction. This produces a completely different type of chlorine−carbon interaction that constrains the geometry of the system along the reaction path (Table 2) and introduces new electronic effects that result in faster thermolysis than the unsubstituted β-hydroxyl aldehyde.

Conclusions

The activation energies and rate constants for the thermolysis of β-hydroxyl aldehydes have been calculated at the MP2/6-311++G(d,p)//MP2(FC)/6-31G(d) level to be between 32 and 38 kcal/mol and 0.8×10^{-5} and 1×10^{-3} s^{-1}, respectively. These results indicate that the thermolysis of β-hydroxyl aldehydes is slower than the thermolysis of similar β-hydroxyl ketones. The B3LYP method with the same basis set underestimates the activation energies and overestimates the rate constants for the thermolysis of the β-hydroxyl aldehydes, in agreement with previous results reported for β-hydroxyl olefins.[9] The inclusion of the effect of tunneling on the rate constants does not change the trend obtained from the uncorrected rate constants but shows clearly the different roles that C_3 and C_4 play in the thermolysis and the effects of substituents.

The AIM analysis in terms of ring critical points and the topology of the electron density shows that the transition state for the thermolysis of β-hydroxyl aldehydes is a six-membered cycle. Furthermore, ρ at the ring critical points is a good criterion for predicting the trends of the thermolysis rates in the β-hydroxyl aldehydes substituted at C_3. On the other hand, the analysis of the electrostatic interaction between O_1 and H_6 accounts for the trends of the thermolysis rates in the β-hydroxyl aldehydes substituted at C_4.

A positive inductive effect due to methyl groups, either at C_3 or C_4, accelerates the reaction with respect to the unsubstituted β-hydroxyl aldehyde; the effect at C_4 is greater than at C_3. A negative inductive effect due to chlorine at C_3 retards the thermolysis rate. However, with chlorine at C_4, the rate of thermolysis is accelerated, and some anomalous results are exhibited.

Acknowledgment. The authors acknowledge Dr. Chérif F. Matta for useful suggestions and comments about this work. The financial support of the Natural Sciences and Engineering Research Council of Canada is gratefully acknowledged.

References and Notes

(1) Smith, G. G.; Yates, B. L. *J. Org. Chem.* **1965**, *30*, 2067.
(2) Yates, B. L.; Quijano, J. *J. Org. Chem.* **1969**, *34*, 2506.
(3) Rotinov, A.; Chuchani, G.; Machado, R. A.; Rivas, C.; Quijano, J.; Yepes, M. S.; Restrepo, I. *Int. J. Chem. Kinet.* **1992**, *24*, 909.
(4) Yates, B. L.; Quijano, J. *J. Org. Chem.* **1970**, *35*, 1239.
(5) Viola, A.; MacMillan, J. H.; Proverb, R. J.; Yates, B. L. *J. Am. Chem. Soc.* **1971**, *93*, 6967.
(6) Notario, R.; Quijano, J.; Quijano, J. C.; Gutiérrez, L. P.; Suárez, W.; Sánchez, C.; León, L.; Chamorro, E. *J. Phys. Chem. A.* **2002**, *106*, 4377.
(7) Quijano, J.; Notario, R.; Chamorro, E.; León, L. A.; Sánchez, C.; Alarcón, G.; Quijano, J. C.; Chuchani, G. *J. Phys. Org. Chem.* **2002**, *15*, 413.
(8) Notario, R.; Quijano, J.; León, L. A.; Sánchez, C.; Quijano, J. C.; Alarcón, G.; Chamorro, E.; Chuchani, G. *J. Phys. Org. Chem.* **2003**, *16*, 166.
(9) Quijano, J.; David, J.; Sánchez, C.; Rincón, E.; Guerra, D.; León, L.; Notario, R. *J. Mol. Struct.* **2002**, *580*, 201.
(10) Chamorro, E.; Quijano, J.; Notario, R.; Sanchez, C.; Leon, L.; Chuchani, G. *Int. J. Quantum Chem.* **2003**, *91*(5), 618.
(11) Dominguez, R.; Rotinov, A.; Chuchani, G.; Quijano, J.; Valencia, C.; Vicente, B.; Franco, D. Actualidades de Físico-Química Orgánica [based on the Latin American Conference on Physical Organic Chemistry], 4th Florianopolis, Brazil, August 1998: pp 348−355.
(12) Chuchani, G.; Dominguez, R.; Rotinov, A.; Quijano, J.; Valencia, C.; Vicente, B.; Franco, D. *J. Phys. Org. Chem.* **1999**, *12* (1), 19.
(13) Laidler, K. J., *Chemical Kinetics*, 3rd ed.; Harper Collins Publishers: New York, 1987.
(14) Atkins, P. W. *Physical Chemistry*, 6th ed.; Oxford University Press: New York, 1998.
(15) Eckart, C. Phys. Rev. **1930**, *35*, 1303.
(16) Shin, H. *J. Chem. Phys.* **1963**, *39*, 2934.

(17) Wigner, E. *J. Chem. Phys.* **1937**, *5*, 720.
(18) Bell, R. P. *The Tunnel Effect in Chemistry*; Chapman and Hall: New York, 1980.
(19) Truhlar, D. G.; Isaacson, A. D.; Skodje, R. T.; Garrett, B. C. *J. Phys. Chem.* **1982**, *86*, 2252.
(20) Truong, T. N.; Truhlar, D. G. *J. Chem. Phys.* **1990**, *93*, 1761.
(21) Truong, T. N. *J. Phys. Chem.* **1997**, *101*, 2750.
(22) Bader, R. F. W.; Essen, H. *J. Chem. Phys.* **1984**, *80*, 1943.
(23) Bader, R. F. W. *Atoms in Molecules—A Quantum Theory*; Oxford University Press: New York, 1990.
(24) Bader, R. F. W. *Chem. Rev.* **1991**, *91*, 893.
(25) Bader, R. F. W. *J. Phys. Chem. A.* **1998**, *102*, 7314.
(26) Reed, A. E.; Curtiss, L. A.; Weinhold, F. *Chem. Rev.* **1988**, *88*, 899.
(27) Alabugin, I. V.; Manoharan, M.; Peabody, S.; Weinhold, F. *J. Am. Chem. Soc.* **2003**, *125*, 5973.
(28) Mitrasinovic, P. *Can. J. Chem.* **2003**, *81*, 1.
(29) Frisch, M. J.; Trucks, G. W.; Schlegel, H. B.; Scuseria, G. E.; Robb, M. A.; Cheeseman, J. R.; Montgomery, J. J. A.; Vreven, T.; Kudin, K. N.; Burant, J. C.; Millam, J. M.; Iyengar, S. S.; Tomasi, J.; Barone, V.; Mennucci, B.; Cossi, M.; Scalmani, G.; Rega, N.; Petersson, G. A.; Nakatsuji, H.; Hada, M.; Ehara, M.; Toyota, K.; Fukuda, R.; Hasegawa, J.; Ishida, M.; Nakajima, T.; Honda, Y.; Kitao, O.; Nakai, H.; Klene, M.; Li, X.; Knox, J. E.; Hratchian, H. P.; Cross, J. B.; Adamo, C.; Jaramillo, J.; Gomperts, R.; Stratmann, R. E.; Yazyev, O.; Austin, A. J.; Cammi, R.; Pomelli, C.; Ochterski, J. W.; Ayala, P. Y.; Morokuma, K.; Voth, G. A.; Salvador, P.; Dannenberg, J. J.; Zakrzewski, V. G.; Dapprich, S.; Daniels, A. D.; Strain, M. C.; Farkas, O.; Malick, D. K.; Rabuck, A. D.; Raghavachari, K.; Foresman, J. B.; Ortiz, J. V.; Cui, Q.; Baboul, A. G.; Clifford, S.; Cioslowski, J.; Stefanov, B. B.; Liu, G.; Liashenko, A.; Piskorz, P.; Komaromi, I.; Martin, R. L.; Fox, D. J.; Keith, T.; Al-Laham, M. A.; Peng, C. Y.; Nanayakkara, A.; Challacombe, M.; W. Gill, P. M.; Johnson, B.; Chen, W.; Wong, M. W.; Gonzalez, C.; Pople, J. A. *Gaussian03*, Revision B.01; Gaussian Inc.: Pittsburgh, PA: 2003.
(30) Brown, R. L. *J. Res. Natl. Bur. Stand. (U.S.)* **1981**, *86*, 357.
(31) Biegler-König, F. W.; Bader, R. F. W.; Tang, T. *J. Comput. Chem.* **1982**, *3*, 317.
(32) Gillespie, R. J.; Bytheway, I.; DeWitte, R. S.; Bader, R. F. W. *J. Inorg. Chem.* **1994**, *33*, 2115.
(33) Solomons, T. W. G. *Organic Chemistry*; Wiley: New York, 1980.
(34) Smith, M. B.; March, J. *March's Advanced Organic Chemistry: Reactions, Mechanisms and Structure*, 5th ed.; Wiley: New York, 2001.
(35) Bader, R. F. W.; Larouche, A.; Gatti, C.; Carroll, M. T.; MacDougall, P. J.; Wiberg, K. B. *J. Chem. Phys.* **1987**, *87*, 1142.
(36) Wiberg, K. B.; Bader, R. F. W.; Lau, C. D. H. *J. Am. Chem. Soc.* **1987**, *109*, 1001.
(37) Mora-Diez, N.; Alvarez-Idaboy, J. R.; Boyd, R. J. *J. Phys. Chem. A.* **2001**, *105*, 9034.
(38) Griffiths, D. J., *Introduction to Electrodynamics*; Prentice-Hall: Englewood Cliffs, NJ, 1999.